*J. Earth Syst. Sci.* (2020)129 56
https://doi.org/10.1007/s12040-019-1326-z


# Mapping of basement structure beneath the Kohima Synclinorium, north-east India via Bouguer gravity data modelling

Ch Ravi Kumar[1], N Kesiezie[1], B Pathak[1], Saumen Maiti[2,*] and R K Tiwari[3]

[1]*Geological Survey of India (GSI), NER, Shillong 793 006, India.*
[2]*Indian Institute of Technology (Indian School of Mines), Dhanbad 826 004, India.*
[3]*CSIR–National Geophysical Research Institute, Hyderabad 500 007, India.*
**Corresponding author. e-mail: saumen@iitism.ac.in*

MS received 3 January 2018; revised 18 October 2019; accepted 29 October 2019

Kohima Synclinorium is one of the most tectonically active corridors of Indian subcontinent and displays complex tectonics of the region. Mapping the basement structure beneath the Kohima Synform is, therefore, vital to provide deep insight into the understanding of the crucial thrust geometry of the region. The vertical gravity gradient anomalies and available geological evidences suggest that the underlying area is occupied by thrust geometry embedded with prominently known tectonic trends of Schuppen Belt (SB), Kohima–Patkai Synclinal (KS–PS) and adjoining Inner Fold Belts (IFB). By keeping in view the massive complex tectonic upheaval in the region, we carried out 2D Bouguer gravity data analysis using the radially averaged power spectral techniques and GMSYS modelling to map the basement depth more precisely. Our results suggest that there is a wide range of heterogeneity in the underlying undulating basement indicating an average sedimentary thickness of the order of 2.2–5.5 km. The gravity PDEPTH modelling results show that source depth varies from 2.5 to 6.5 km. There is an uplifted basement tending towards the southwestern part while gradual deepening of basement was observed towards the eastern part of the study area. The profile modelling results show the presence of basement in a depth range of 2.5–3.8, 3.8–4.0, and 3.8–4.2 km beneath Foreland Basin (FB), Kohima–Patkai Synclinal structures (KS–PS), and Inner Fold Belts (IFB), respectively. The underlying results of integrated profiles, PDEPTH and GMSYS modelling would be useful to understand the detailed basement structure and tectonic trends of Belt of Schuppen (BS), Kohima–Patkai Synclinal structures (KS–PS) and adjacent Inner Fold Belts (IFB) of north-eastern region of India.

**Keywords.** Tectonic structures; basement depth; Kohima Synclinorium; north-eastern region; Bouguer gravity anomalies; PDEPTH and GMSYS modelling.

## 1. Introduction

Geologically the north-eastern region (NER) of the Indian subcontinent comprises six distinct tectonic zones, viz., Eastern Himalayan collision zone, Mishmi block of Himalayan Arc and Myanmar Arc, Indo-Myanmar subduction zone or Mobile belt, Assam–Brahmaputra valley, Meghalaya plateau and Bengal basin (Verma and Mukhopadhyay 1977; Nandy 1980; Mukhopadhyay 1984; Kayal

Published online: 22 January 2020

1987; Kayal and Zhao 1998; Acharyya *et al.* 1990; Khan 2005). The NER of India lies at the junction of Himalayan Arc to the north and Myanmar Arc to the east. The collision of Indian plate and Eurasian plate involves the large-scale active continental deformation and therefore, a rather diffuse seismicity prevails in this region (Kayal 1996; Nandy 2001; Khan 2005). The geology of NER is well studied compared to geophysical studies, and tectonic models have been proposed by several researchers (Mathur and Evans 1964; Verma *et al.* 1976; Dasgupta 1977; Mukhopadhyay 1984; Rao 1983; Acharyya 1991). The present study area, Kohima Synclinorium exists well within the Indo-Burmese mobile belt Range (IBR) covered with distinct lithological and structural characteristics of accretionary prism/complex. The basement structure of Kohima Synclinorium remains a matter of considerable speculation due to terrain difficulties. In particular, mapping of basement structure, geosynclinals sediment thickness, understanding thrust geometry of Belt of Schuppen (BS), Kohima–Patkai Synclinal structures (KS–PS) and adjacent Inner Fold Belt (IFB) configurations are very important. Here we have taken up a task based on gravity data analysis augmented by efficient spectral analysis techniques to map basement structure beneath Kohima Synclinorium and surrounding areas.

The main objectives of this paper are to (i) interpret Bouguer gravity anomalies with subsurface geology, in order to decipher the basement heterogeneity and overlying geosynclinal sediment thickness; and (ii) understand the nature of subsurface thrust geometry and tectonic trends of Kohima Synclinorium and adjoining areas.

Bouguer gravity data have been used for addressing the above problems of local/regional tectonic setting and for mapping of the basement structures. The basement depth imaging of the entire study region was determined by using the moving windows averaging technique of gravity data (Spector and Grant 1970; Naidu 1972; Naidu and Mathew 1988, 1998). The vertical gravity gradient anomalies, PDEPTH modelling along Werner depth solutions of the selected profiles and GMSYS modelling results supplemented with seismic data give comprehensive insight into the concealed thrust geometry and tectonic trends of Belt of Schuppen (BS), Kohima–Patkai Synclinal structures (KS–PS) and adjacent Inner Fold Belts (IFB) of NER.

## 2. General geology and tectonics of the study area

The present study area, comprising of the north-east India lies between the spatial coordinates 25°–27°N latitude and 93°–95°E longitude (figure 1). The area under the study can be broadly classified into four tectonic zones. The western parts are occupied by Precambrian shield of Mikir massif, which represents an uplifted detached block of Shillong plateau composed of granitoid gneiss of Early Proterozoic age ($\sim$2.5 Ga) with acid and basic intrusive, it is also imprinted with several lineaments and rectilinear drainage pattern (Dasgupta and Biswas 2000; Nandy 2001). The Mikir Massif is surrounded by Assam Foreland Basins (FB) with varying litho-units of sediments. The north-western part of the study area is covered by Surma and Tipam sedimentary rocks. The Disang and geosynclinal facies of the Barail sedimentary rocks make up the south-eastern part of the study area. These two litho units are separated by the BS, which is a series of imbricate thrust slices

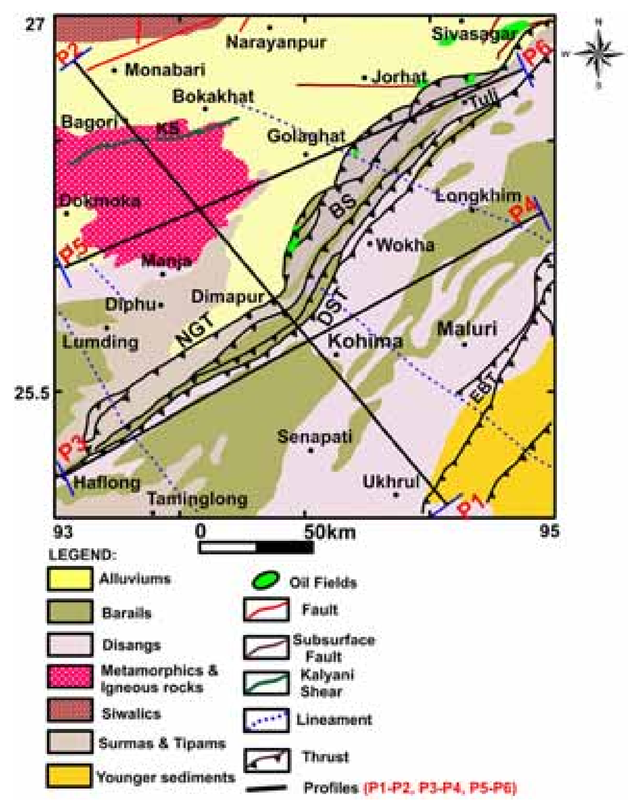


Figure 1. Simplified geological map of Kohima Synclinorium, north-east India (modified after Dasgupta 1977). Abbreviations. NGT: Naga Thrust, DST: Disang Thrust, BS: Belt of Schuppen, EBT: Eastern Boundary Thrust zone, KS: Kalyani Shear.

trending northeast–southwest direction comprises of Naga Thrust (NGT) and Disang Thrust (DST) belts. The BS forms the outermost fringe of Assam–Arakan basin in the eastern parts of the study area (figure 1). This entire zone is subjected to intense thrusting and sedimentation with complex structure overriding one over the other. It marks a south-eastern boundary of Assam plains and extends along the western limb of KS–PS (Evans 1964). The Kohima belongs to the morphotectonic subdivision of Assam–Arakan tertiary folded and thrust belts also known as the IFB. The IFB mainly comprises of outer wedge of the IBR with structural complexity and terrain difficulties running almost NNE–SWW direction. This includes north Cachar hills, Laimatol-Mizo hills and extends up to the Tripura fold belts. The study area is occupied by two synform structures, the Kohima Synclinorium in the south and Patkai Synclinorium in the north (Dasgupta and Biswas 2000; Srinivasan 2007).

## 3. Methodology

In the present study, we have applied signal processing techniques (e.g., second vertical derivative, 2D radially averaged power spectrum, PDEPTH modelling using Werner Deconvolution technique, and 2D gravity modelling) to Bouguer gravity data to understand the basement heterogeneity and overlying geosynclinal sediment thickness of Kohima region. Second order vertical derivative (VDR) of Bouguer gravity anomalies (Elkins 1951; Marson and Klingele 1993; Murthy 1998) was used to enhance shallow subsurface anomalies obscured by broader regional trends and to outline the edges of source bodies and litho-logical boundaries over Kohima Synclinorium.

Two-dimensional (2D) radially averaged power spectrum was calculated over Kohima Synclinorium to estimate the depth to the top of the interface with varying density contrast to the basement. The Bouguer gravity data have been transformed in Fourier domain using equivalent layer concept. Here the first order gravity spectrum at the surface caused due to subsurface layer with relief spectrum $\Delta h(k)$, depth $h_0$ and density contract $\Delta\rho$ in 2D can be interrelated (Spector and Grant 1970; Naidu 1972; Mishra and Pederson 1982; Mishra 2011).

$$\Delta g(k) = 2\pi G \Delta\rho e^{-2\pi|k|h_0} \Delta h(k). \quad (1)$$

The power spectrum of equation (1) can be expressed as:

$$|\Delta g(k)|^2 = 4\pi^2 G^2 \Delta\rho^2 e^{-4\pi|k|h_0} |\Delta h(k)|^2. \quad (2)$$

Taking natural logarithm in both sides of equation (2), we can write as

$$\ln\langle|\Delta g(k)|^2\rangle = -4\pi h_0|k| + \ln(4\pi^2 G^2 \Delta\rho^2 \langle|\Delta h(k)|^2\rangle). \quad (3)$$

In equation (3), $\langle\ \rangle$ denotes radial average (Spector and Grant 1970). The above equation can be approximated as a straight line with slope $-4\pi h_0$ in that $h_0$ may be found by plotting the natural logarithmic power spectrum against the wavenumber, $|k|$.

The gravity basement depths were computed by employing moving window averaging technique based on radially averaged power spectrum (Spector and Grant 1970; Naidu and Mathew 1988). In that a small and suitable window size slides over a large gridded gravity data with some overlap for computing radially averaged power spectrum of various windows choosing appropriate pass and cut-off wavelengths of gravity data.

'PDEPTH' modelling using Werner Deconvolution technique (Werner 1953; Hartman *et al.* 1971) is an iterative 2D inversion scheme to find the horizontal position and depth of causative source body from profile gravity data. The unknown parameters to define the anomalies are estimated by Marquardt's least-squared inversion method (Ku and Sharp 1983). The method allows estimating depth solutions and the geometry of different gravity source bodies using a series of moving window along the profile (Mammo 2012).

## 4. Qualitative analysis of Bouguer gravity

The original Bouguer gravity anomaly map of the study region (GSI–NGRI 2006), covering an area of 45,000 km$^2$ was re-sampled with a pixel size of 1 km$^2$ (figure 2). The gravity anomaly map has brought out varying gravity anomaly pattern over different lithological units and shows an overall variation of –179 mGal ranging from maximum value of 40 mGal over the southwest part and minimum of –219 mGal observed over the northeast portion. Based on the gravity variation, the study area can be classified into three distinct gravity anomalous zones, viz., high (H), low

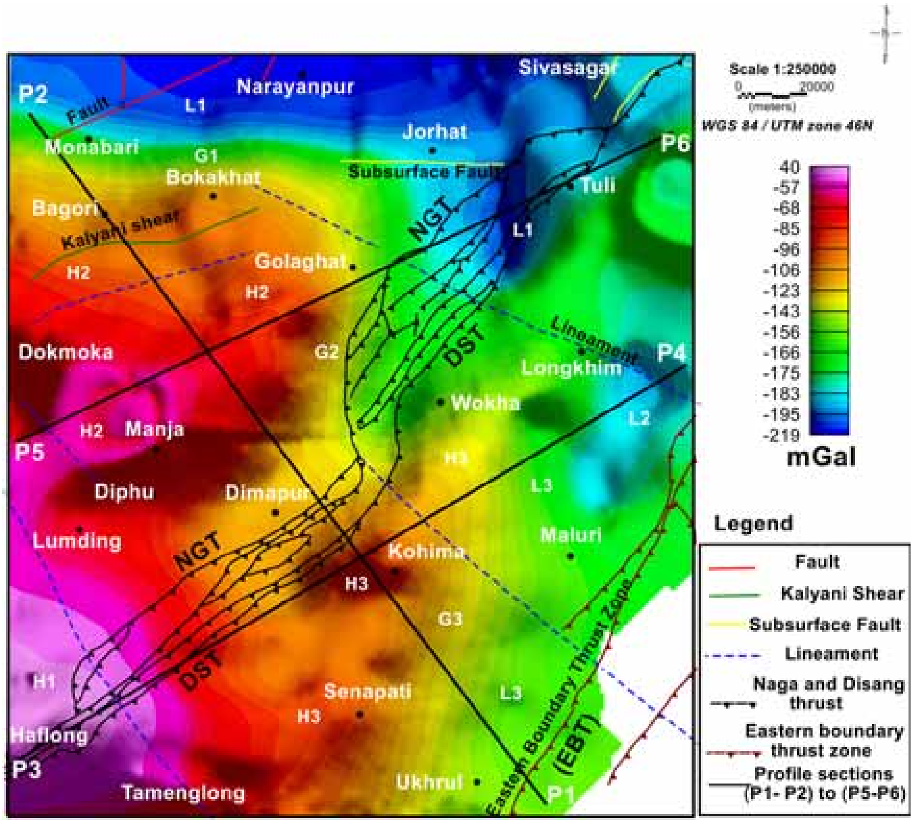


Figure 2. Bouguer gravity anomaly map of north-east India overlain with tectonic features such as Naga Thrust (NGT) and Disang Thrust (DST). The zones of gravity high are marked as H1, H2 and H3. The zones of gravity low are denoted as L1, L2 and L3. The zones of fault signatures in terms of horizontal gravity gradients are represented as G1, G2 and G3. P1–P2, P3–P4 and P5–P6 are selected profiles.

(L) and gradient (G) zones (figure 2). The Bouguer gravity anomaly map shows that southwestern part is characterized by gravity high (H1). This gravity high (H1) is attributed to either high-density mafic and/or ultramafic rocks or basement up-warping. A significant broad high anomaly (H2) noticed over exposed Mikir Massif represents an uplifted block, which is composed of granitoid gneiss with acid and basic intrusive (Dasgupta and Biswas 2000). Moderately high gravity (H3), trending along NE–SW direction extends from south of Senapati to Kohima (figure 2). An east–west trending strong gravity low (L1) has been characterized by Assam Fore Land Basin and Siwalik formation (figure 2). This anomaly extends further south-east of Jorhat to Belt of Schuppen (BS). NGT and DST have been interpreted from Bouguer anomaly plot (figure 2). Northeast–southwest trending isolated gravity low (L2) is characterized by IFB. Northeast to southwest trending moderately low gravity anomaly (L3), has been interpreted in terms of a possible intense compression (folded) and/or thrusting caused by the presence of thick low density sediments (figure 2). It is an important structural element at the eastern boundary thrust belt of Indo-Burma Range (IBR) subduction zone (Kayal 1996). The relative gravity low anomalies over basement depressions are due to the thick underlying sedimentary column. The major northeast–southwest trending moderate gravity anomalies are sandwiched between the zones of BS, that merely coincide with the NGT and DST (figure 2). These thrust belts are not a single plane throughout, rather it is made up of a succession of different thrusts (Evans 1964; Srinivasan 2007). The Bouguer gravity anomaly map represents two striking features. One of them is identified by steep gravity gradient (G1) trending east–west which delimits the northern boundary and the other one is northeast trending gravity gradient (G2), which is characterized by the outer edge of the Mikir Massif nearing to the Brahmaputra fore-land basin (FB). The north–south trending gravity gradient (G3) clearly distinguishes the Kohima Synclinorium from IFB. These steep gravity gradients could be due to deep seated faults and/or litho-logical contacts. The study area is cutting across several major lineaments trending NNW–SSE, NW–SE and NWW–SEE directions, which bisects the northeast–southwest trending NGT and DST (figure 2). A NEE–SWW trending lineament parallel to the Kalyani shear zone, cut across Mikir Massif. The gradual decrease of gravity from north to northeastern part of upper Assam valley could be attributed to deepening of basement from north to north-east (Verma and Mukhopadhyay 1977).

## 5. Vertical derivative map of Bouguer gravity data

The second order vertical derivative map has been used to enhance local anomalies obscured by broader regional trends and to delineate edges of source bodies and/or litho-logical boundaries (Elkins 1951; Marson and Klingele 1993; Murthy 1998; Ajayakumar *et al.* 2017). We have computed second vertical derivative of Bouguer gravity anomaly of the study area. This map enhances several local anomalies masked by the broader regional gravity trends and brought out near circular anomaly due to outer edge of the Mikir Massif (figure 3). The pronounced east–west trending anomaly at southwestern part of the study area marks the boundary of the southern extension of the imbricated thrust belt (figure 3). The near circular anomaly pattern, as is evident from the image could be linked to high-density mafic/ultramafic rocks and/or basement up-warping. The prominent northeast–southwest trending negative anomalies with discrete nature represent distinct tectonic features of BS. This may be due to the underlying sediments of varying thickness under intense folding and thrusting.

A striking north–south to northeast–southwest trending high gravity vertical gradient anomaly observed from Senapati to Tuli, which is characterized by geosynclinal sediments at Kohima and Patkai. The moderately low gradient anomalies are characterized by Assam–Arakan folded and thrusts belts/IFB. To understand the nature of the underlying basement and sedimentary thickness of the highly complex folded and thrust belts, five selective profile sections (S1–S2 to S9–S10) were considered for present examination. The results of each profile are discussed separately for the interpretation of tectonic belts of BS, synclinal structures and IFB.

## 6. Quantitative analysis of Bouguer gravity data

### 6.1 *Spectral analysis of Bouguer gravity data*

The Bouguer gravity data were transformed in the frequency domain to compute 2D radially averaged power spectra. The averaged radial spectra provide the depths estimate of the causative sources at the different gravity interfaces (Spector and Grant 1970; Naidu 1972; Radhakrishna *et al.* 2002; Singh *et al.* 2004; Mishra 2011). The slope of the logarithmic power spectrum of Bouguer gravity anomaly gives the ensemble average depth of the corresponding causative bodies due to density contrast. The computed spectrum *vs.* wave number (figure 4) provides three straight line segments. The depths corresponding to 20.92 km (deeper layer interface), 8.66 km (middle layer interface) and 4.46 km (shallow layer interface) are associated with the gravity anomaly of longer, moderate and shorter wavelength, respectively (figure 4). The deeper interface depth of 20.92 km attributed to the lower crust. The other two interface depths indicate the upper crustal and the basement depth beneath the Kohima Synclinorium and its surrounding areas (figure 4). It may be noted that line segment data points of logarithmic power spectrum are fitted with straight line. The slope is derived by fitting it to the line segment data using least-squared techniques. Selection of data points in each cluster may give rise to different slopes resulting in a range of probable depths instead of a single depth. This has permitted us to calculate an appropriate statistical uncertainty bound of the depth estimates. Accordingly, we have experimented with different data points from each line segments and ascertain the depth along with its uncertainty bound. We found excellent correlation (co-efficient of determination $\sim$0.90) in all the depth estimations, including upper and lower bound. However, we accepted the basement depth solution with highest co-efficient of determination ($\sim$0.98) (table 1). The average computed basement depths beneath the Kohima Synclinorium have been found within the uncertainty bounds ($\sim\pm$ 0.50 km) (table 1).

### 6.2 *Gravity basement depth imaging map*

The gravity basement depth imaging map (figure 5) shows that undulation in the gravity basement depth varies from 2.2 to 4.1 km. These basement depths were computed by using the moving window

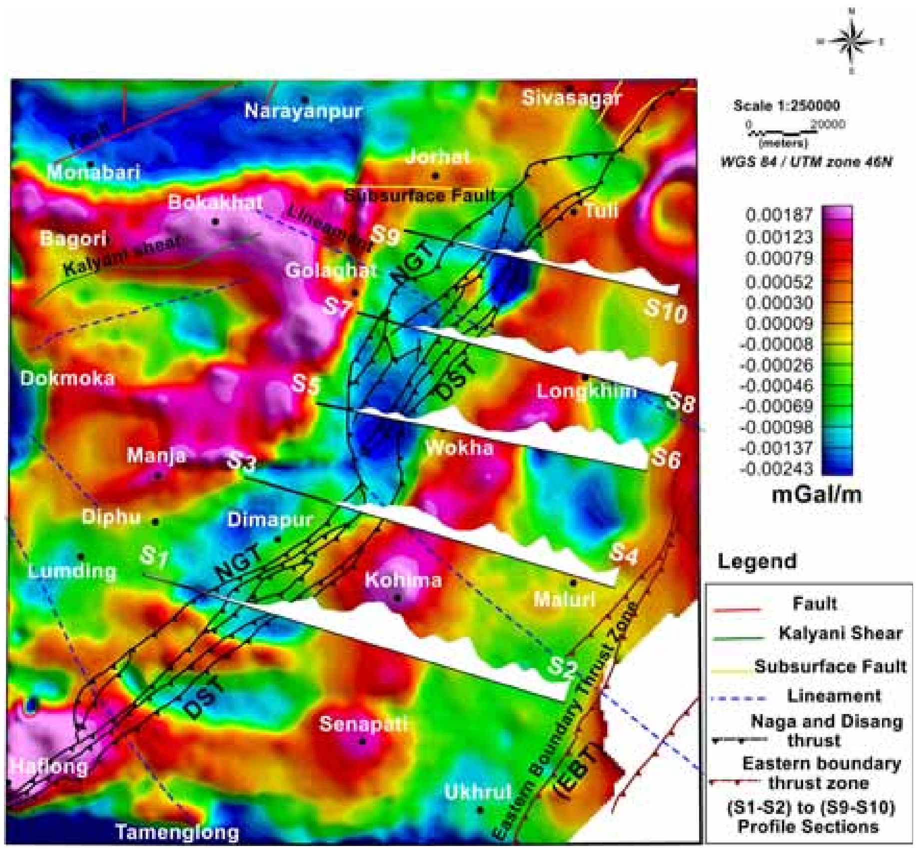


Figure 3. Vertical derivative (VDR) anomaly map derived from Bouguer gravity data of north-east India is overlain with tectonic features. Five profiles (S1–S2, S3–S4, S5–S6, S7–S8, and S9–S10), which cut across different tectonic features are shown.

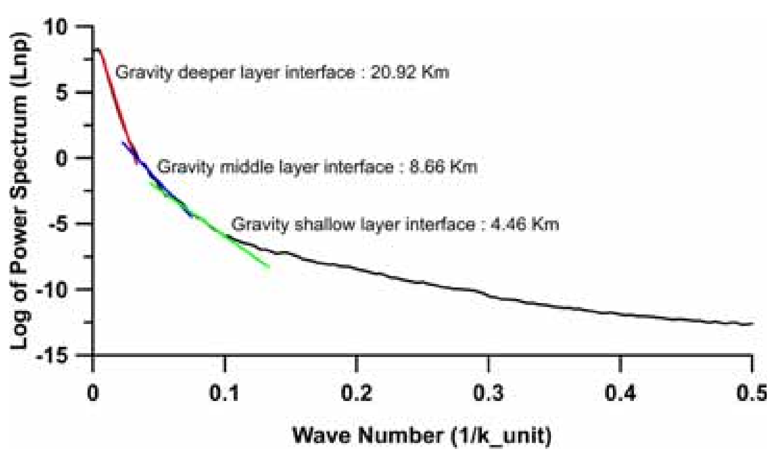


Figure 4. Bouguer gravity based (figure 2) spectral analysis results for study region in north-east India.

Table 1. *Estimation of basement depth uncertainty from spectral analysis of gravity data.*

| Slope of line segment | Estimated depth (km) | Coefficient of determination | Depth uncertainty (km) |
|---|---|---|---|
| Lower bound | 3.93 | 0.967 | −0.53 |
| Mean | 4.46 | 0.973 | ∼±0.50 |
| Upper bound | 4.94 | 0.981 | +0.48 |

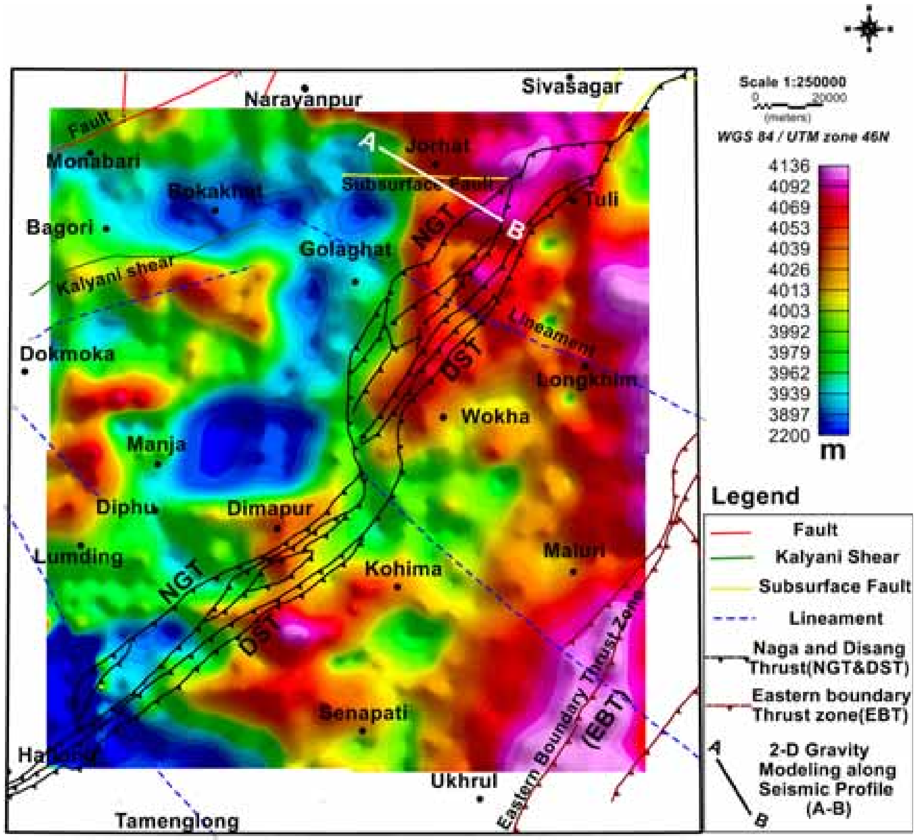


Figure 5. Bouguer gravity based basement depth map of the study region. The western part of basement depth map reveals shallow basement while eastern part indicates gradual deepening of basement.

averaging technique based on radially averaged power spectrum (Spector and Grant 1970; Naidu and Mathew 1988, 1998). A small and suitable window (15 km ×15 km) slide over a large grid of gravity data with 5% overlap for computing radially averaged power spectrum of several windows based on appropriate pass and cut-off wavelengths shows depth variations from 2.2 to 4.1 km. These depths are very useful in understanding the relative vertical movement of various segments of gravity basement. Deeper basement depths are depicted in the eastern and northeastern parts of arcuate shaped north-south trending Eastern Boundary thrust and IFB (figure 5). There is an uplifted basement towards southwest of the study area, pronounced circular shallow basement structure is noticed around Mikir Massif and west of Golaghat areas. Moderate basement depths were estimated in rest of the portion of the study area (figure 5).

### 6.3 *PDEPTH – Modelling of basement using Werner method*

To understand the signatures of the different exposed geological formations and geotectonic units, three Bouguer gravity profiles were selected, viz., P1–P2, P3–P4, and P5–P6 over the gravity grid. The northwest–southeast directed profile (P1–P2) is characterized by the low gravity region of eastern boundary thrust zone, across NGT and DST, with moderately high over Kohima Synclinorium and Mikir Massif. Further north, gravity profile cuts across low gravity zone towards north-western portion over Brahmaputra FB. An uplifted basement is proposed along profile (P3–P4) to explain the gravity high at the southwestern part of the study area. The profile (P3–P4) cuts across imbricated thrust zone and Kohima region. Towards east prominent low and isolated gravity anomaly is centered over IFB. The profile (P5–P6) is passing through Mikir Massif and extending up to northeast of Golaghat. Thrust and IFB are characterized by gravity low along the profile (P5–P6). We employed 'PDEPTH' modelling using Werner deconvolution technique (Werner 1953; Ku and Sharp 1983) to compute gravity source depth along the gravity profiles following Hartman *et al.* (1971).

Accordingly, the estimated depth solutions derived from the Werner deconvolution technique is shown (figure 6a–c). The Werner deconvolution technique

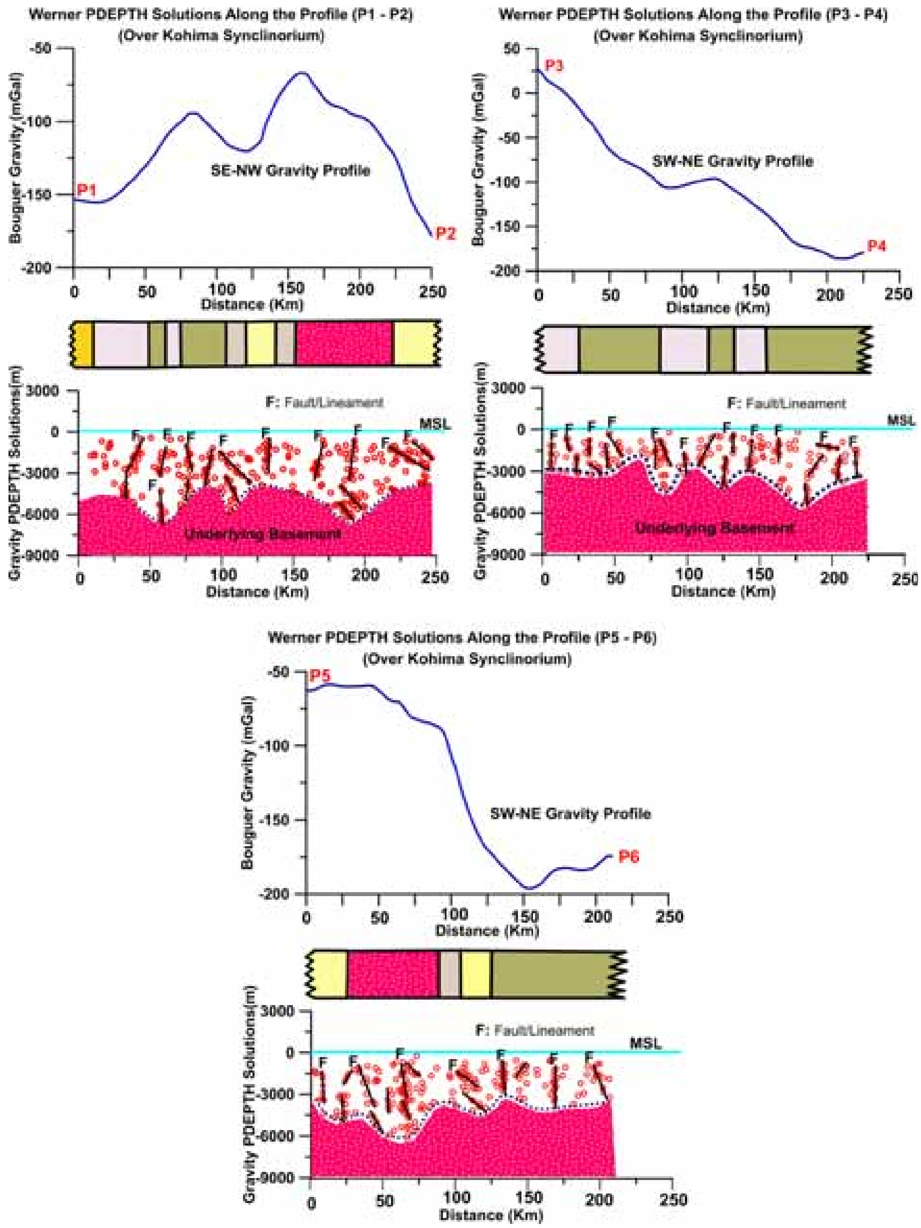


Figure 6. Werner PDEPTH modelling results along three profiles (P1–P2, P3–P4, P5–P6) which cuts across Kohima Synclinorium (legend is same as in figure 1).

(Werner 1953) essentially searches for variations in slope and curvature. The PDEPTH as employed here allows recognizing potential anomalies and automatically computing their horizontal and vertical location, depth, anomalous density contrast and geometry. The clusters of Werner depth solutions provide source depth variations along the profiles over Kohima Synclinorium and surrounding areas. The source depths are found to be varied from 2.5 to 6.5 km (figure 6a–c). Deeper depth solutions are characterized by density variation with respect to basement at deeper depths. The Werner based depth solutions and their clustering pattern provide important clue to the interpretation/delineation of fault/lineament (F) of the study region. The variations of depth to the basement represent how sediment thickness varies along the three regional profiles. These Werner PDEPTH solutions are in well agreement with the depths obtained by spectral analysis and basement depth imaging techniques of gravity data.

### 6.4 *Profile sections (S1–S2, S3–S4, S5–S6, S7–S8, and S9–S10) across Kohima Synclinorium and adjoining areas*

The vertical derivative map of gravity data brings out the geometry of thrust tectonics of complex

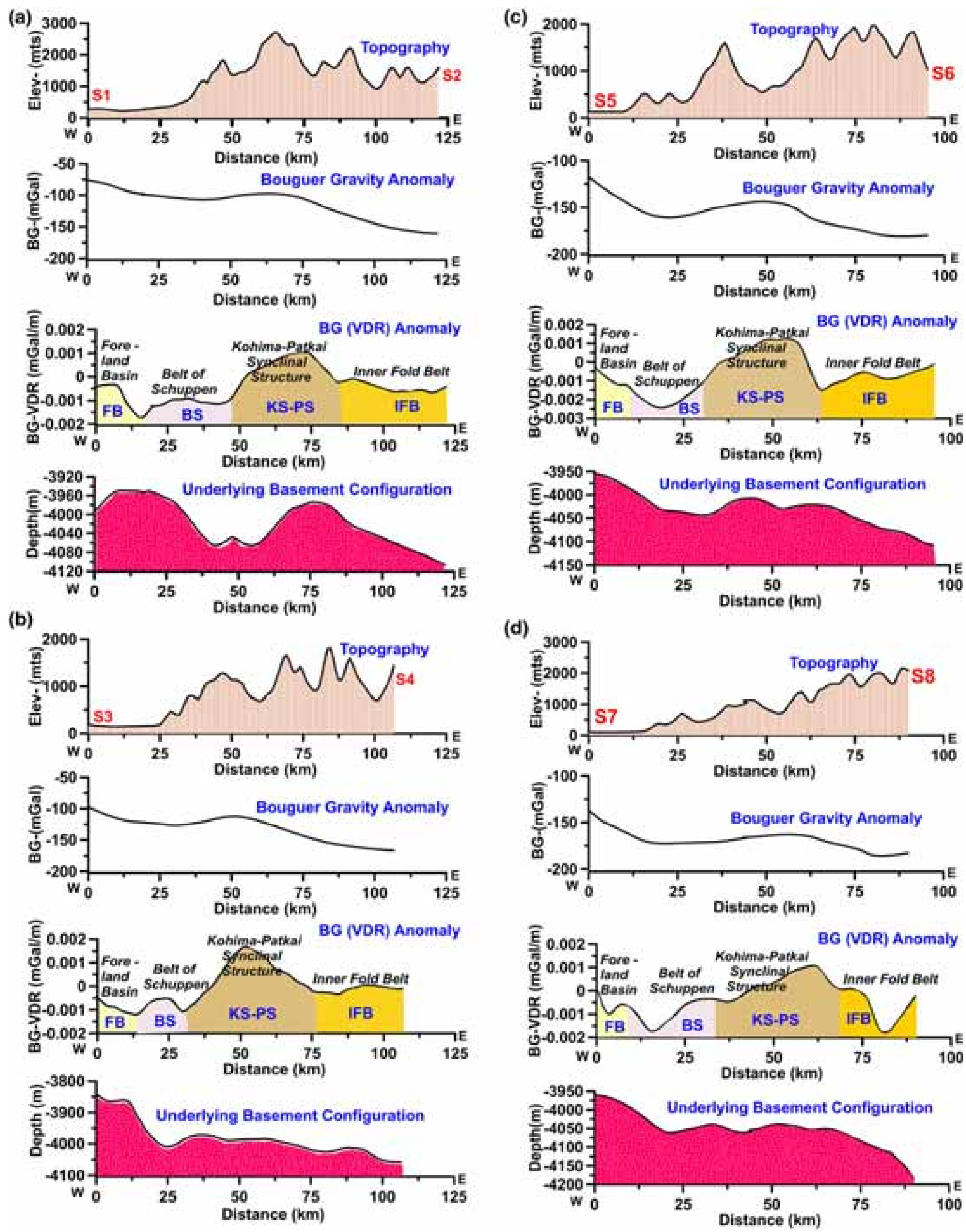


Figure 7. (**a–e**). The integrated profiles along S1–S2, S3–S4, S5–S6, S7–S8, and S9–S10 (figure 2 for locations). These plots reflect the influence of lithology and basement configuration of foreland basin on gravity and their vertical derivatives.

NER. Five profiles (S1–S2, S3–S4, S5–S6, S7–S8, and S9–S10), which cuts across the distinct geological formations and tectonic elements of Kohima Synclinorium and adjoining areas (figure 7a–e) were considered along east–west direction for the present analysis. These profile sections exhibit nature of the topographical variations, Bouguer gravity anomalies, second vertical derivative of Bouguer gravity responses and underlying basement configuration along with their association with tectonics and subsurface geology. Particularly, Bouguer gravity and its vertical derivative anomalies differentiate among the various lithological boundaries of fore land basin, BS, KS–PS structure adjacent to IFB (figure 7a–e). These results demonstrate lateral variation of underlying basement and thickness of the sediments. It depicts that western part over FB is likely to have shallow basement, whereas the adjacent thrust belt, KS–PS and IFB are interpreted to be relatively deeper

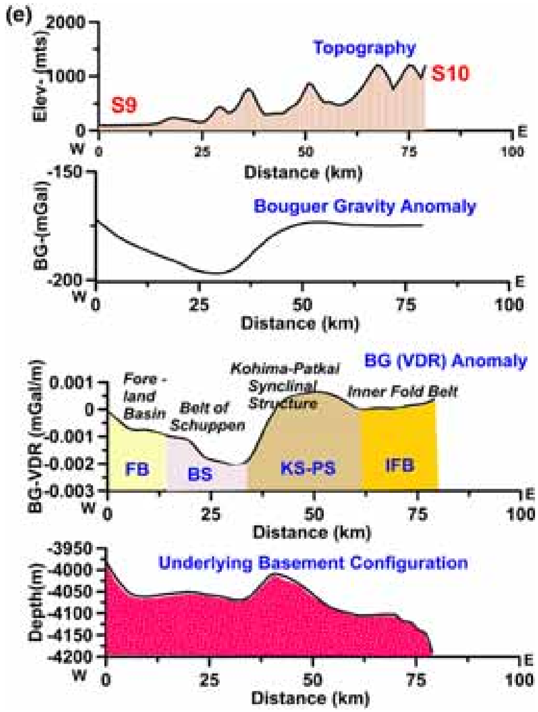


Figure 7. (*Continued.*)

undulating basement, suggesting intense folding and thrusting over geosynclinal sediments. The inferred basement depth results indicate gradual basement deepening towards the east (Verma and Mukhopadhyay 1977).

### 6.5 *Gravity 2D subsurface modelling (GMSYS) along the profile sections (AB)*

We generated 2D subsurface gravity model along profile (AB) using GMSYS module of Geo-soft to understand different geological formations. These include Assam foreland basins, imbricated thrust of BS zone and adjacent Assam–Arakan IFB. The selected profiles were modelled by constraining the available seismic depth results (e.g., sedimentary thickness), and gravity interface depths (figure 8a–b).

The observed gravity anomaly yields a fairly good match with the computed curve with RMS error of 0.9. Modelling results suggest underlying basement's gradual deepening towards east with undulations. The basement depth varies from 2.2 to 5.5 km. Shallow basements are characterized by foreland basins whereas the deep basements are inferred beneath BS. The computed results are in good agreement with the seismic depth section (figure 8b) as well as drilling data (Saha 2012).

## 7. Discussion

A broad high gravity anomaly zone over Mikir Massif represents an uplifted block composed of granitoid gneiss of Early Proterozoic age ($\sim$2.5 Ga) with acidic and basic intrusive (Dasgupta and

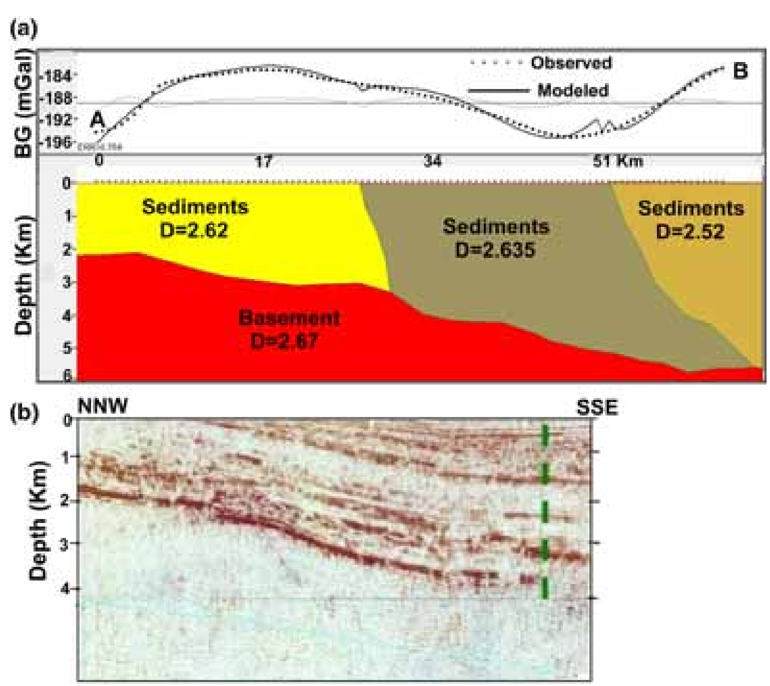


Figure 8. (**a**) A 2-D gravity model for profile A–B (figure 2) and it cuts across the foreland basin, a belt of Schuppen zone. (**b**) A limited seismic section (after Saha 2012) is shown in the lower panel.

Biswas 2000). The pronounced east–west trending gravity high demarcates around Haflong (figure 2). The gravity high over the southern extension of the imbricated thrust belt defines basement up-warping and/or presence of high-density mafic/ultramafic rocks. On the other hand, a high gravity anomaly trending almost east–west direction may be due to the southern fringe of the uplifted Shillong plateau or basement ridge, which may be responsible to form a significant east–west trending fault, known as Dauki–Haflong thrust fault (Nandy 2001). The significant low gravity outlines upper Assam and FB. Thrust geometry is characterized by moderately low gravity and second vertical derivative anomalies. The discrete isolated gravity lows over BS represents, undulating nature of the basement and accumulation of thick sediments (figure 5). The BS is one of the prominent morphotectonic features of northeastern region, which is composed of Tertiary sediments. The BS has undergone more than eight over thrust (Evans 1964; Srinivasan 2007). At BS, the response of gravity and second vertical derivative with discrete nature indicate that thickness of the underlying sediments has undergone intense folding and thrusting resulting in undulating basement. The results of profile sections (figure 7a–e) reveal that sedimentary thickness considerably increases below the imbricated thrust belts and adjoin IFB, which is also inferred by 2D gravity modelling results (figure 8a–b) and seismic and drilling information (Saha 2012). Besides the BS, the other major structural units of the study region include north–south to northeast-southeast trending KS–PS synclinal structures, which is clearly depicted by the trends of both gravity and its second vertical derivative signatures. The Kohima Synform structures extend from south-west of Kohima to further south of Senapathi. The Kohima Synclinorium makes northwest contact by the DST. The PS, which is comprised of Barail rocks, are subjected to intense thrust of Disang shale. The PS extends from south of Wokha to northeast of Tuli and it makes contact by the DST (figure 3). The computed basement depths beneath KS–PS are found to be slightly lower than those of adjacent thrust and IFB (figure 5). The nature of the underlying basement and disposition of synclinal sedimentary layer of the complex folded and thrusted belts are delineated from the analysis of PDEPTH modelling. The selected profile sections of the study region are compared with 2D gravity modelling result constrained by available seismic section along the profile (AB). The comparative results are found to be excellent, clearly demonstrating density in-homogeneities along the particular transect (figure 8a–b). Thus, the present analysis based on 2D radially averaged power spectrum with appropriate uncertainty bounds of the estimated depths, second vertical derivatives, PDEPTH modelling combining with Werner deconvolution and 2D gravity modelling along a particular transect supplemented with seismic data provide deeper insights into the basement architecture, the thrust geometry and tectonic trends of Kohima region.

## 8. Summary and conclusions

We have carried out a comprehensive research for the understanding of basement structure and nature of complex tectonic geometry underneath the Kohima Synclinorium and its adjoining inner fold belts from the interpretation of Bouguer gravity data complemented with seismic data. Well established techniques such as 2D radially averaged power spectra, basement depth imaging armed with PDEPTH and GM-Sys modelling were employed to qualitatively and quantitatively characterize the concealed basement heterogeneity and sedimentary thickness. The major conclusions are as follows:

- The Bouguer gravity analysis with qualitative and quantitative interpretation brings out basement structure over Kohima Synclinorium. The results of spectral analysis, basement depth modelling and the Werner PDETH modelling reveal that average sediment thickness in this area varies from 2.2 to 5.5 km with undulating basement.
- The pronounced gravity high is attributed to anomalously high density material underlain by the mafic/ultramafic rocks. The major northeast to south-west nosing gravity anomalies sandwiched between the Schuppen Belt (SB) zones is associated with moderately high gravity anomalies, which are in tune with the Naga Thrust (NGT) and Disang Thrust (DST).
- Analysis reveals that underlying sedimentary thickness has varied possibly due to influence of compression and thrusting. The Werner PDEPTH modelling along selected profiles delineates distinct geological formations and tectonic elements of over Kohima Synclinorium. Combined plot shows the inter-relationship among

Bouguer gravity, its second vertical derivative and various lithological boundaries of Brahmaputra Fold Belts, Belt of Schuppen (BS), and Kohima–Patkai Synclinal structures (KS–PS) adjacent to Inner Fold Belts (IFB).

- The 2D gravity modelling constrained by seismic data suggests the presence of basement in a depth range of 2.2–3.5 km below Brahmaputra Foreland basin and 3.5 to 5.5 km below Belt of Schuppen (BS). Moderately shallow basement over Kohima–Patkai is attributed to synclinal structure. The present results also suggest that the basement deepening towards Inner Fold Belts (IFB), which appears to be of paramount importance as these sedimentary basins may host significant amount of oil deposits in the study area.

## Acknowledgements

SM is thankful to Director, IIT (ISM), Dhanbad, for giving permission to publish this work. Partial financial benefit from the Ministry of Earth Sciences, Govt. of India, New Delhi, India, is also thankfully acknowledged (Grant No: MoES/P.O. (Geosci)/44/2015). RKT thanks to DAE for RRF award. We are thankful to Prof M Radhakrishna, Associate Editor and an anonymous reviewer for providing positive and professional comments to improve the quality of the earlier version of the paper.

## References

Acharyya S K, Ray K K and Sengupta S 1990 Tectonics of ophiolite belt from Naga Hills and Andaman Islands, India; *J Earth Syst. Sci.* **99** 187–199.

Acharyya S K 1991 Late Mesozoic to Early Tertiary basin evolution of the northern and eastern collsion margins of the Indian Plate; *J. Him. Geol.* **1** 75–91.

Ajayakumar P, Rajendran S and Mahadevan T M 2017 Geophysical lineaments of Western Ghats and adjoin coastal areas of central Kerala, southern India and their temporal development; *Geosci. Front.* **8** 1089–1104.

Dasgupta A B 1977 Geology of Assam–Arakan region; *Quart. J. Geol. Min. Met. Soc. India* **49** 54.

Dasgupta A B and Biswas A K 2000 Geology of Assam; *Geol. Soc. India* **57** 169.

Elkins T A 1951 The second derivative method of gravity interpretation; *Geophysics* **16** 29–50.

Evans P 1964 Tectonic framework of Assam; *J. Geol. Soc. India* **5** 80–96.

GSI–NGRI Gravity Map series of India (RGMI – 2006), Geological Survey of India.

Hartman R R, Tesky D J and Friedberg J L 1971 A system for rapid digital aeromagnetic interpretation; *Geophysics* **36** 891–918.

Kayal J R 1987 Microseismicity and source mechanism study: Shillong Plateau, northeast India, *Bull. Seismol. Soc. Am.* **77** 184–191.

Kayal J R 1996 Earthquake source processes in northeast India: A review; *J. Him. Geol.* **17** 53–69.

Kayal J R and Zhao D 1998 Three-dimensional seismic structure beneath Shillong Plateau and Assam valley, northeast India; *Bull. Seismol. Soc. Am.* **88** 667–676.

Khan P K 2005 Mapping of b-value beneath the Shillong Plateau; *Gondwana Res.* **8** 271–276.

Ku C C and Sharp J A 1983 Werner deconvolution for automated magnetic interpretation and its refinement using Marquart's inversion modelling; *Geophysics* **48** 754–774.

Mammo T 2012 Analysis of gravity field to reconstruct the structure of Omo basin in Ethiopia and implications for hydrocarbon potential; *Mar. Petrol. Geol.* **29** 104–114.

Marson I and Klingele E E 1993 Advantages of using the vertical gradient of gravity for 3-D interpretation; *Geophysics* **58** 1588–1595.

Mathur L P and Evans P 1964 Oil in India; International Geological Congress (22nd session), New Delhi, 85p.

Mukhopadhyay M 1984 Seismotectonics of transverse lineaments in the eastern Himalaya and foredeep; *Tectonophys.* **109** 227–240.

Mishra D C and Pederson I B 1982 Statistical analysis of potential fields from subsurface reliefs; *Geophys. Explor.* **19** 247–266.

Mishra D C 2011 Gravity and magnetic methods in geological studies: Principles, integrated exploration and plate tectonics. B.S. Publications, Hyderabad, ISBN: 978-93-81075-27-2.

Murthy I V R 1998 Gravity and magnetic interpretation in exploration geophysics, *Geol. Soc. India Memoir* **40** 356.

Naidu P S 1972 Maximum likelihood (ML) estimation of depth from the spectrum of aeromagnetic fields; *Pure Appl. Geophys.* **95** 141–149.

Naidu P S and Mathew M P 1988 Computed program for radial and angular spectrum estimation; Unpubl. Rep. Geol. Surv. India, AMSE, Bangalore.

Naidu P S and Mathew M P 1998 *Analysis of geophysical potential fields: A digital signal processing approach*; Elsevier, Netherlands, 298p.

Nandy D R 1980 Tectonic pattern in north eastern India; *Indian J. Earth Sci.* **7** 103–107.

Nandy D R 2001 *Geodynamics of northeastern India and the adjoining region*; ACB Publication, Kolkata, 209p.

Radhakrishna M, Verma R K and Purushotham A K 2002 Lithospheric structure below the eastern Arabian Sea and adjoining west coast of India based on integrated analysis of gravity and seismic data; *Mar. Geophys. Res.* **23** 25–42.

Rao A 1983 Geology and hydrocarbon potential of a part of Assam–Arakan Basin and adjacent regions; *Petrol. Asia J.* **6(4)** 127–158.

Saha D 2012 Integrated analysis of gravity and magnetic in the Upper Assam shelf and adjoining Schuppen belt area – A critical review; Extended Abstract Presented at *GEO-India*, Search and Discovery Article # 30228.

Singh A P, Mishra D C, Gupta S B and Rao M R K P 2004 Crustal structure and domain tectonics of the Dharwar

Craton (India): Insight from new gravity data; *J. Asian Earth Sci.* **23** 141–152.
Spector A and Grant F S 1970 Statistical models for interpreting aeromagnetic data; *Geophysics* **35** 293–302.
Srinivasan 2007 Regional structure configuration and seismic pattern of 'belt of Schuppen' in northeast India; *J. Geol. Soc. India* **70** 801–814.
Verma R K and Mukhopadhyay M 1977 An analysis of the gravity field in northeastern India; *Tectonophys.* **42** 283–317.
Verma R K, Mukhopadhyay M and Ahluwalia M S 1976 Seismicity, gravity and tectonics of northeast India and northern Burma; *Bull. Seismol. Soc. Am.* **66** 1683–1694.
Werner S 1953 *Interpretation of magnetic anomalies of sheet-like bodies*; vol. **43,** Sveriges Geologiska Arsbok, Stockholm.

Corresponding editor: Munukutla Radhakrishna